Subsea Flowline-PLET-Jumper Integrated Abaqus Model

Chong Zhou, Xinhai Qi, and Lijuan Wang

Genesis

Abstract*: Oil and gas field development is moving into ever deeper waters to meet the world's growing demand for energy. Subsea flowlines, jumpers and pipeline end terminals (PLETs) are the key components for a reliable and cost-effective subsea field development. Usually, the subsea flowline, jumper and PLET are designed and analyzed separately by different engineering groups using simplified end boundary conditions, and the interface loads from the flowline / jumper to PLET are obtained from de-coupled finite element (FE) models. Due to simplifications, the reactions among different subsea components may be over-estimated, resulting in un-optimized components in certain subsea design. The local stress and strain in pipes may also be over-predicted, especially when a large PLET pitch angle as per specified installation tolerances is considered for design. This paper presents a comprehensive Abaqus model to more accurately analyze the subsea system collectively. The integrated Abaqus model including the flowline, PLET, jumper, and seabed is first discussed in details. Then, a case study with typical subsea design inputs is performed, considering the installation, hydrotest, operation, and full shutin loading conditions. It is observed from the Abaqus results that the proposed numerical model can more effectively and accurately simulate the interactions among subsea components; therefore, it may be cost-effective to consider this methodology in subsea system design.*

Keywords*: Subsea, Flowline, PLET, Jumper, Integrated Model, Finite Element Analysis, Interface Loads.*

1. Introduction

Large thermal expansion is expected at the ends of subsea production flowlines due to the high temperature and high pressure loads introduced from deep water reservoir fluids. PLETs with sliding capability and M shape vertical steel jumpers are typically employed to absorb the large displacement load at the flowline ends. To maximize the sliding capacity, the M shape jumpers are arranged nearly perpendicular to the flowline. The special coating material Teflon is usually applied to the contact area between the PLET sliding module and sliding rails to minimize the sliding resistant force. Distributed buoyancy modules along the flowline can be used to initiate lateral buckles and increase flowline fatigue life if needed. Figure 1.1 shows a typical subsea tie-back system used to manage the large flowline expansion during operation. If severe flowline walking (i.e., axial ratcheting over various operational cycles) is predicted, an anchoring system is required at a flowline end to control such movement, mitigating the risk of jumper overstress failure.

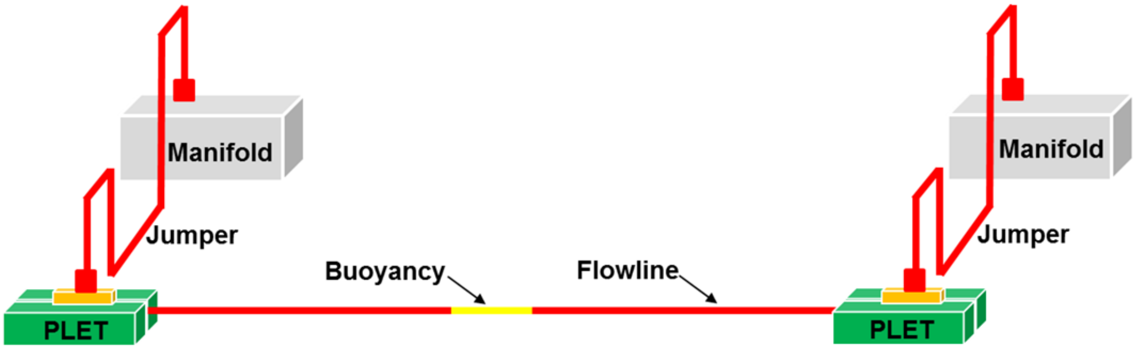

Figure 1.1 Typical Flowline / PLET / Jumper System Schematic

Usually, the subsea flowline, jumper and PLET are designed and analyzed separately by different engineering groups using simplified end boundary conditions. The interface loads from the flowline / jumper to PLET are obtained in de-coupled FE models.

In a jumper FE model, the jumper connector at the manifold side is treated as fixed since the relatively rigid manifold is usually restrained by a suction pile to the seabed. For the jumper connector at the sliding PLET side, the displacement load due to flowline expansion is applied as a boundary condition in one degree of freedom (DOF), while the other five DOFs are fixed. Such simplified jumper boundary conditions may result in a larger reaction bending moment and higher pipe stress because the PLET foundation stiffness is not considered and any jumper end rotation is neglected. For jumpers with small span lengths, the simplified boundary conditions may be acceptable for the jumper design. However, for jumper with large span lengths (which is likely driven by large flowline end movement), the big reaction moment from the de-coupled model can overstress the jumper pipe at the ends, which may lead to an artificial design failure.

A similar situation exists for the de-coupled flowline model as well. In a de-coupled flowline model, only the flowline and seabed are simulated with pipe elements and rigid quadrilateral elements respectively. A contact pair is defined between flowline and seabed surface. The complex pipe-soil interaction can be described with a friction user subroutine. However, at the end of the flowline, simplified boundary conditions are used to represent the interaction between the flowline and sliding PLET, as shown in Figure 1.2. The flowline end is offset a short distance (approximately 2ft) vertically from the seabed to represent the separation between the flowline/PLET bulkhead interface and the PLET mudmat foundation. Along the flowline direction, the displacement restraint is released while a frictional resistant force is applied at the flowline end to represent the PLET sliding resistance. The lateral displacement in the direction perpendicular to the flowline and the other three rotational displacements are typically fixed.

The de-coupled flowline model cannot accurately capture PLET sliding resistance because the jumper reaction force varies with jumper connector position. Furthermore, if the PLET has a pitch angle, the total flowline end resistant force during expansion will be different from that during contraction since a gravity component of the PLET sliding module will contribute to the total resistance. More importantly, de-coupled models may over-estimate bending moment and pipe stress/strain at the flowline/jumper ends since the deformation of PLET foundation and PLET structure is not considered. The over-estimated reaction loads at the flowline/jumper ends are subsequently provided to the detailed PLET design. This may lead to over-sized subsea structures and hence increased fabrication / transportation / installation costs.

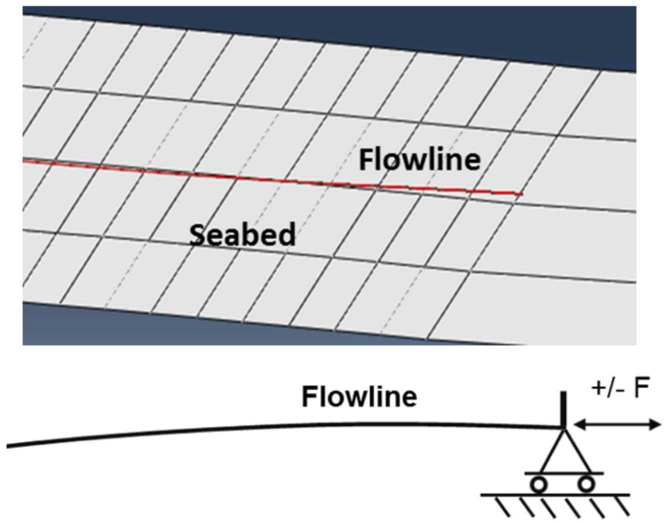

Figure 1.2 De-coupled Flowline FE Model

To optimize the design of the subsea flowline system, a flowline-PLET-jumper integrated model is created to investigate the interface loads and pipe stress/strain at flowline/jumper ends. The details of the integrated model are presented in the next section.

2. Integrated Model

Deep water subsea flowlines generally have PLETs at their ends (1st end PLET and 2nd end PLET depending on pipe-lay direction), which are welded to the flowline offshore and lowered to the seabed through the moon pool or from a support structure on an installation vessel. The moon pool size and / or the load capacity of handling devices impose a limitation on the PLET dimensions and weight. A properly designed PLET can sometimes be vital for the subsea system in terms of cost and installation feasibility.

To improve the understanding of the subsea system behaviors, a nonlinear integrated Abaqus model has been developed to analyze the flowline, PLET and jumper collectively. The integrated model considers soil-pipe interaction, PLET mudmat-soil interaction, seabed undulations, PLET sliding mechanism, PLET structural stiffness, jumper stiffness, and installation tolerance.

2.1 Finite Element Model

The integrated model is illustrated in Figures 2.1 through 2.3. Two-node pipe elements are used to model the nominal flowline and jumper pipe. The thick-walled pipe element option, introduced in the Abaqus 6.12-1 version, is utilized in the finite element model. It not only accounts for the variation of the hoop and radial stress through pipe wall thickness due to the pressure loads, but also better predicts the axial expansion response of pipes with large wall thickness-to-radius ratios under high temperature and pressure loading. The long flowlines are meshed with 4ft long pipe elements, while the jumpers have a 1 ft mesh density. Four-node quadrilateral rigid elements are utilized to construct the discrete rigid surface simulating the three-dimensional (3D) uneven seabed. The soil-pipe interactions are simulated by a contact pair with load-deflection curves of axial and lateral soil resistances defined by an in-house Abaqus user subroutine for non-linear contact behavior.

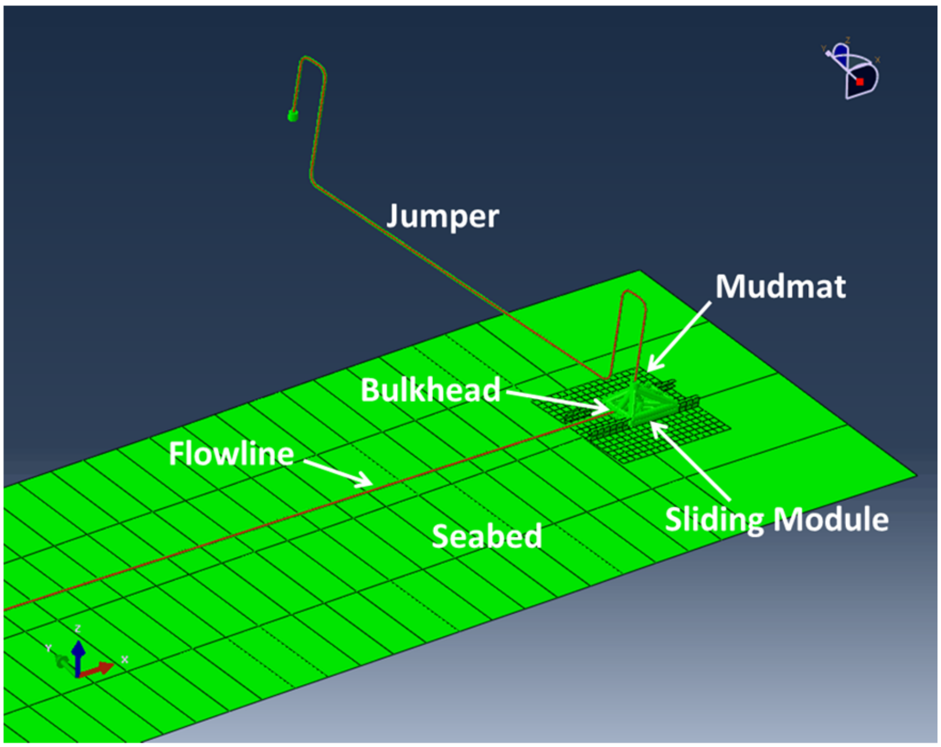

Figure 2.1 Subsea Flowline-PLET-Jumper Integrated Model

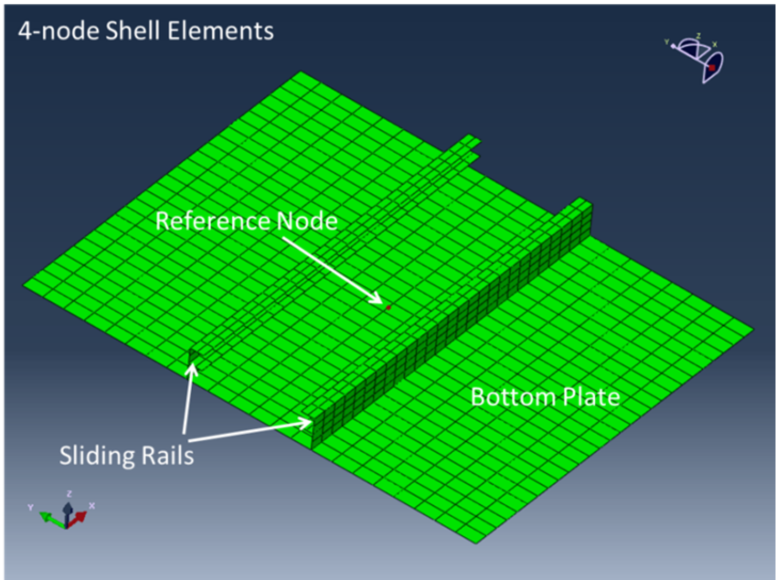

Figure 2.2 PLET Mudmat-Soil Interaction

Four-node shell elements are used to model the PLET mudmat with two sliding rails, as shown in Figure 2.2. A distributed coupling constraint is defined between the mudmat bottom surface and a center reference node, which is connected to three transitional and three rotational soil springs. The interaction between PLET mudmat and soil is represented by the properly defined soil spring stiffness.

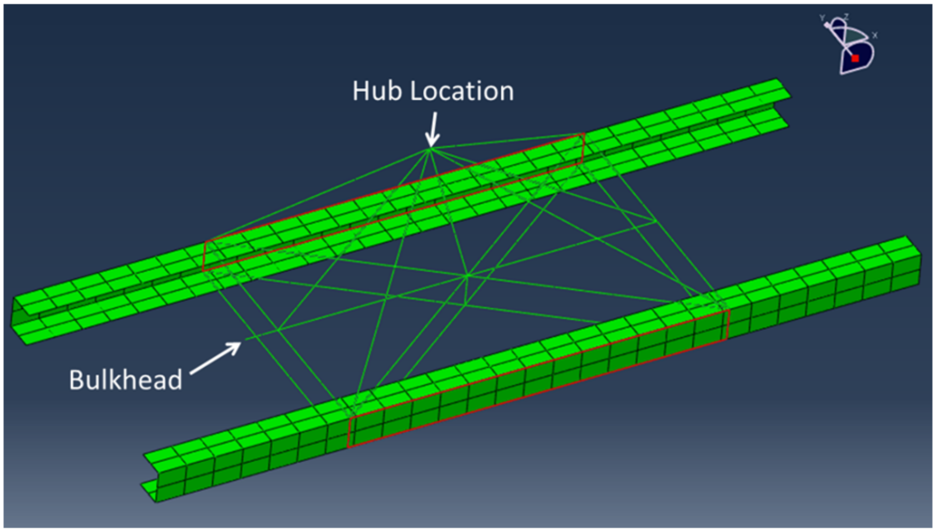

Figure 2.3 PLET Sliding Module

As shown in Figure 2.3, the sliding module is simplified by a frame structure with general beam elements, reflecting the overall structural stiffness from the PLET design (detailed PLET structure analysis is not in the scope of present paper). The jumper hub location needs to be accurately modeled to ensure that the mudmat bending moment transferred from jumper reactions is correct. The weight of the sliding module is applied such that it travels with the PLET sliding module while the pipe end expands and contracts. Contact pairs are defined between the sliding rail surfaces and the beam element surfaces in red to simulate the PLET sliding mechanism, as shown in Figure 2.3. The friction coefficient of the contact pairs can be adjusted to match the actual test data of the sliding friction force.

Usually, one end of a jumper structure is rigidly connected to a PLET hub while the other end is connected to a hub of a relatively rigid manifold sitting on an anchor pile. Thus, the jumper end at the manifold side moves very little once installed and is treated with fixed boundary conditions in the integrated model shown in Figure 2.1.

2.2 Load Steps

A typical loading sequence for the flowline-PLET-jumper integrated model is listed in Table 2.1.

Table 2.1 Loading Sequence of Integrated Model

<table>
<tr><th>Step No.</th><th>Description of Major Analysis Steps</th></tr>
<tr><td colspan="2">As-laid Condition</td></tr>
<tr><td rowspan="3">1-3</td><td>Establish flowline on flat seabed</td></tr>
<tr><td>Lower the flowline to uneven seabed to set up contact</td></tr>
<tr><td>Set boundary conditions at the PLET</td></tr>
<tr><td colspan="2">Flooded Condition</td></tr>
<tr><td>4</td><td>Flood the pipe and apply hydrostatic pressure</td></tr>
<tr><td>5</td><td>Connect jumper to PLET</td></tr>
<tr><td colspan="2">Hydrotest Condition</td></tr>
<tr><td>6</td><td>Apply hydrotest pressure to flowline and jumper</td></tr>
<tr><td>7</td><td>Reduce to the hydrostatic pressure – depressurize</td></tr>
<tr><td colspan="2">Initial Start-Up (Design) Condition</td></tr>
</table>

Step No.	Description of Major Analysis Steps
8	Apply operational weight and the design temperature/pressure
9	Reduce to the shut-in pressure and ambient temperature – shutdown
Operation / Shutdown Cycles	
Cycles	Apply the operational pressure / temperature
	Apply the pressure / temperature of various shutdown cycles

3. Design Data

A case study is performed using the flowline-PLET-jumper integrated model. The input data for the design example are described in this section.

3.1 Environment Data

A typical deep water environment is used for the case study. The water depth is assumed to be 5,000 ft. The average seawater density is 64 lb/ft^3 over the water column. The ambient temperature at the seabed is 39°F.

3.2 Flowline-PLET-Jumper Design Data

The geometry data and material properties of the flowline/jumper pipe used in the design example are summarized in Table 3.1.

Table 3.1 Pipe Geometry and Material Data

Parameter	Unit	Data
Nominal Outside Diameter	in	10.75
Pipe Wall Thickness	in/mm	1.063/27
External Insulation Thickness	in	2.5
External Insulation Density	lb/ft^3	62.4
Flowline Length	ft	14,000
Jumper Span Length	ft	124.0
Submerged Weight (Empty)	lb/ft	68.1
Submerged Weight (Flooded or Hydrotest)	lb/ft	94.2
Submerged Weight (Operation)	lb/ft	92.4

Parameter	Unit	Data
Specified Minimum Yield Strength of Steel (X70)	psi	70,000
Specified Minimum Tensile Strength of Steel	psi	82,000
Young's Modulus of Elasticity	psi	2.9×10^7
Poisson's Ratio	-	0.30
Steel Density	lb/ft^3	490.0
Thermal Expansion Coefficient	/ ^oF	6.5×10^{-6}
Content (Production) Density	lb/ft^3	60.0

The PLET mudmat overall size is selected to be 27 ft x 30 ft. The total PLET submerged weight is 93,300 lbf, including the 34,400 lbf sliding module and 58,900 lbf PLET mudmat. The submerged weight of the jumper connector is taken as 2,300 lbf. The PLET sliding resistance force is assumed to be approximately 13,000 lbf at the neutral position.

The hydrotest pressure, design pressure, maximum pipeline operating pressure and temperature are tabulated in Table 3.2.

Table 3.2 Temperature and Pressure Loads of Pipeline

Parameter	Unit	Data
Design Pressure @ Mean Sea Level (MSL)	psig	9,000
Hydrotest Pressure @ MSL	psi	11,250
Maximum Operating Pressure @ MSL	psig	8,000
Hydrostatic Pressure (5,000 ft water depth)	psi	2,236
Topside Shut-in Pressure	psig	3,200
Maximum Operating Temperature	^oF	140

3.3 Soil Properties

Very soft clay with undrained shear strength of 25 psf is assumed for the case study. The transitional and rotational soil stiffness of the PLET mudmat foundation can be calculated by the formulas proposed by Gazetas (1991), assuming the rotation center is at the mudmat geometry center. However, under a large bending moment, the situation of mudmat-soil partial contact might exist and the empirical equations for bending stiffness may not be applicable. Given the equivalent vertical stiffness, a separate local FE mudmat-soil model with multiple compression only soil springs is generated to calculate the foundation bending stiffness under the combined loads, as shown in Figure 3.1.

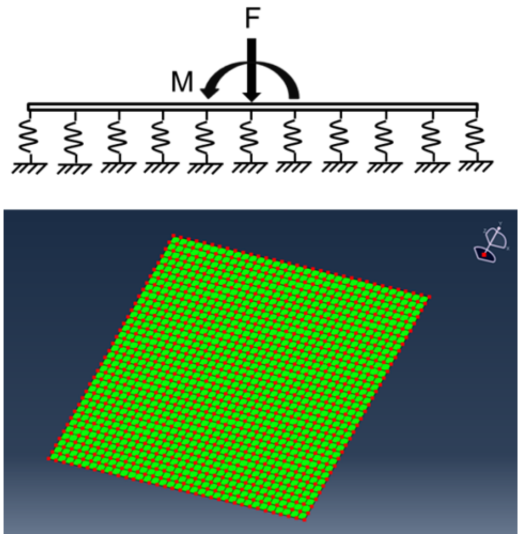

Figure 3.1 Abaqus Muli-Spring Mudmat-Soil FE Model

The calculated stiffness in Table 3.3 is applied to the PLET foundation of the integrated model for the case study. The x axis in Table 3.3 is parallel to flowline direction, while the y axis is perpendicular to flowline and z axis is the vertical direction.

Table 3.3 PLET Foundation Stiffness

Soil Spring Stiffness	Unit	Value
K_z (Vertical Transitional Stiffness)	kip/in	43.4
K_y (Lateral Transitional Stiffness)	kip/in	31.2
K_x (Axial Transitional Stiffness)	kip/in	31.7
K_{rx} (Rotational Stiffness in Roll Direction)	kip-in/Rad	499,859
K_{ry} (Rotational Stiffness in Pitch Direction)	kip-in/Rad	407,705
K_{rz} (Torsional Stiffness)	kip-in/Rad	2,460,698

Although not shown herein, a comparison was made between the simplified soil multi-spring model above and a comprehensive 3D soil model that considers non-linear soil properties. It is found that the results of the integrated model based on the two PLET-soil models for the case under investigation are very close. The multi-spring model is more conservative in terms of interface load and pipe stress / strain if the applied load is greater. For instance, under a large bending moment the pipe end may rotate substantially based on the 3D soil model with consideration of non-linear soil properties. This results in more reduction in the interface load and pipe stress / strain in the PLET span as compared to the soil multi-spring model.

3.4 PLET Pitch Angle

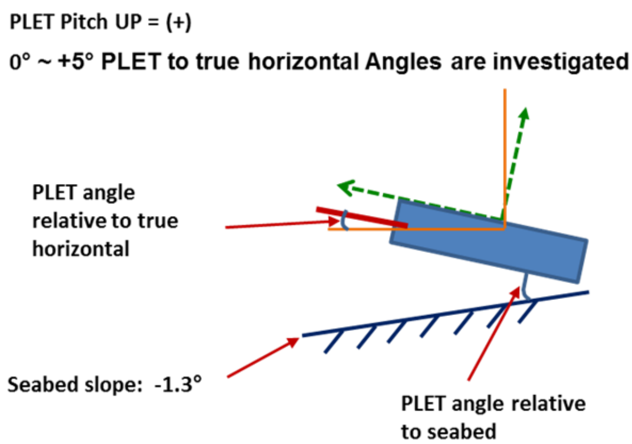

Figure 3.2 Seabed Slope and PLET Pitch Angle

The pitch angle of PLETs has an important influence on flowline end span length and bending moment. If the PLET pitches up, namely the PLET flowline side is higher as shown in Figure 3.2, the flowline end span length and bulkhead bending moment increase. To account for installation tolerance, PLET pitch angles from 0° to 5° relative to true horizontal are investigated. With the -1.3° seabed slope assumed in the model, the PLET relative to seabed pitch angle studied varies from 1.3° to 6.3°.

4. Results and Discussions

As shown in Figure 4.1 and Figure 4.2, the flowline end bending moment and pipe strain increase with the PLET pitch angle relative to the seabed. Due to the PLET foundation stiffness and PLET structural stiffness being included in the integrated model, flowline end rotation and vertical displacement are expected to cause a reduction on the bending moment and pipe strain when compared to the de-coupled flowline model with simplified boundary conditions.

It is observed that the depressurized condition has the largest flowline end bending moment due to the tensile flowline axial force, but the design condition has the worst pipe strain at the flowline end due to thermal loading. Figure 4.1 and Figure 4.2 show that the reduction in bending moment at the flowline end (or PLET bulkhead) is in the range from 13% to 20%, while the reduction in maximum pipe strain at the flowline end varies from 8% to 13%, depending on the PLET pitch angle. The flowline end rotates 0.77° and lowers 3.5 inch at the depressurized condition. The reduction in the interface load and pipe strain will be greater if the flowline end is allowed to rotate and move more by using less conservative stiffness of soil and / or PLET structure in the analyses.

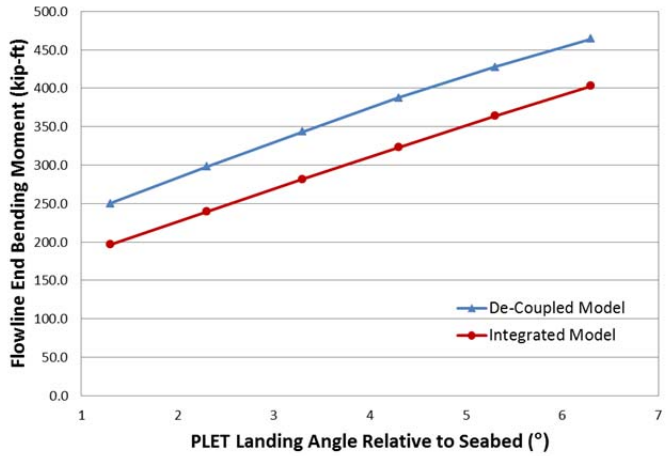

Figure 4.1 Flowline End / Bulkhead Bending Moment (Depressurized Condition)

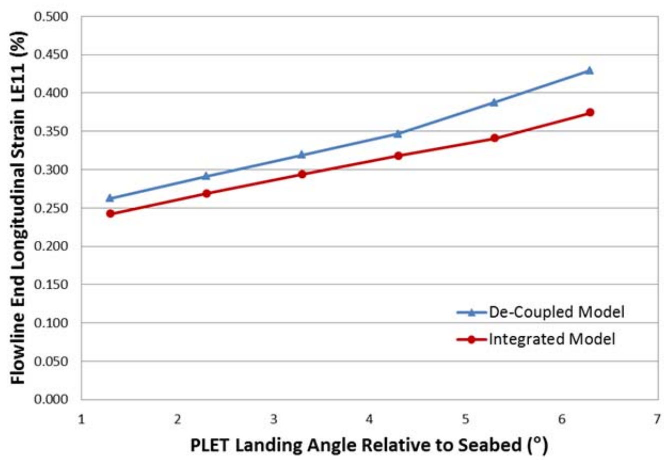

Figure 4.2 Maximum Flowline End Pipe Longitudinal Strain (Design Condition)

Table 4.1 tabulates the maximum pipe stress at the flowline end under various loading scenarios, assuming a 0° PLET pitch angle. The comparison shows that the integrated model can reduce the pipe stress level from 4% to 20% if the flowline end movement is considered. For the hydrotest and the design operating conditions, the stress reduction is minor because the pipe stress due to internal pressure dominates. The depressurized and the cooldown conditions have the greatest stress reduction since the pipe stress at the flowline ends is mainly introduced by bending moment which decreases with flowline end rotation.

Table 4.1 Flowline End Pipe Stress with Horizontal PLET

Maximium Flowline End Von Mises Stress (ksi)					
Load Step	**As-Laid**	**Hydrotest**	**Depressized**	**Design**	**Cooldown**
De-Coupled Model	35.9	63.6	41.7	54.2	42.5
Integrated Model	30.3	61.2	33.4	52	34.9
Difference	16%	4%	20%	4%	18%
Maximium Flowline End Longitudinal Stress (ksi)					
Load Step	**As-Laid**	**Hydrotest**	**Depressized**	**Design**	**Cooldown**
De-Coupled Model	41.5	57.7	43.1	52.9	44.9
Integrated Model	35.5	51.3	34.8	48.1	36.9
Difference	14%	11%	19%	9%	18%

The reduction of pipe stress and bending moment above the jumper connector at the PLET side is also observed in the integrated model, although the difference is not as significant as that of the flowline end due to the relatively large mudmat-soil bending stiffness in the jumper plane.

Unlike the traditional de-coupled models, where flowline end reactions and jumper end reactions have to be manually combined involving conversion of coordinate systems, the final equivalent loads on the PLET mudmat can be directly outputted from the six soil springs of the integrated model for PLET mudmat sizing.

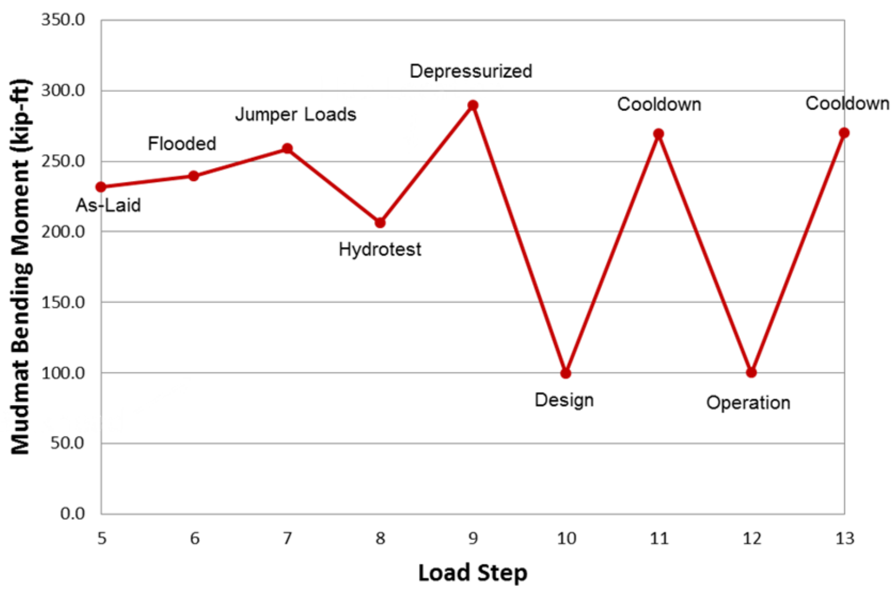

Figure 4.3 Total Bending Moment on Mudmat in PLET Pitch Direction

Figure 4.3 shows the combined mudmat bending moment in the PLET pitch direction (around the axis perpendicular to the flowline) under different loading scenarios. As the PLET sliding module travels along the PLET sliding rails, the PLET equivalent CG shifts and the location of jumper / flowline end reaction forces moves as well, causing a fluctuation of the total bending moment on the mudmat foundation. Generally, the largest mudmat bending moment is expected at the depressurized or cooldown condition as the flowline contracts, while the smallest mudmat bending moment is expected at the design or operation condition as the flowline expands.

5. Conclusions

De-coupled subsea flowline /jumper models may overestimate the flowline-PLET or jumper-PLET interface loads and stress in structure components, leading to less efficient or non-cost-effective design of the subsea system. To improve the understanding of the global behavior of the subsea system under various loading scenarios, an integrated model has been developed to analyze the subsea flowline-PLET-jumper system collectively.

By incorporating the PLET foundation stiffness and the PLET structural stiffness, the integrated model may generate more accurate loads at the flowline to PLET interface and pipe stress / strain at flowline/jumper ends. Therefore, the integrated model may be cost effective for optimizing subsea system design.

6. References

1. Gazetsa, George, “Formulas and Charts for Impedances of Surface and Embeded Foundations,” Journal of Geotechnical Engineering, Vol. 117, No. 9, Sep. 1991.
2. API RP 2A WSD, “Recommended Practice for Planning, Designing and Constructing Fixed Offshore Platforms,” 21st Edition, Dec. 2000.
3. Verruijt, Arnold, “Offshore Soil Mechanics”, Delft University of Technology, 2005
4. Abaqus Users Manual, Version 6.12-1, Dassault Systémes Simulia Corp., Providence, RI.